Supplementary Material

Neglect battery

Patients underwent a paper-and-pencil neglect battery [1] including a line bisection test consisting in eight lines horizontally disposed in a vertical A4 sheet in a fixed random order (three 60 mm samples, three 100 mm samples and two 180 mm samples)[2]; three cancellation tests in which patients were asked to cancel stimuli of various sort: (1) lines[3], (2) As among other letters[4], (3) silhouettes of bells among other objects[5]; an overlapping figures task[6], in which patients where requested to identify five patterns of overlapping linear drawings of common objects (one central and a pair of objects over each of its sides); a copy of a linear drawing representing a central house and four trees (a pair of trees over each of its side) presented on a horizontal A4 sheet[19].

MRI acquisition

MRI data were acquired using echo-planar imaging at 1.5T (General Electric) with a standard head coil for signal reception. DTI axial slices were obtained using the following parameters: repetition time, 6575ms; echo time, 74.3ms; flip angle, 90°; matrix, 128 x 128 ; slice thickness, 4mm with no gap; FOV, 28 cm; acquisition time, 250s . One average was used with signal averaging in the scanner buffer. Diffusion weighting was performed along 36 independent directions, with a b-value of 700s/mm2. High-resolution 3-D anatomical images were used for display and anatomical localization (114 axial contiguous inversion recovery three dimensional fast SPGR images, 1.2mm thick; inversion time, 450ms; flip angle, 15°; matrix, 256 x 256; FOV, 28cm; acquisition time, 370s).

Diffusion Tensor Data Analysis

Data were analysed on an independent workstation (Linux PC, kubuntu 6.06 LTS). Raw diffusion-weighted data were corrected for geometric distortion secondary to eddy currents using a registration technique based upon the geometric model of distortions[7]. Brainvisa 3.0.2 (http://brainvisa.info/) software was used to calculate diffusion tensors and anisotropy data, define the ROIs and perform fibre tracking.

Tractography

Fibre tracking of the superior longitudinal fasciculus (SLF), inferior longitudinal fasciculus (ILF) and the inferior fronto-occipital fasciculus (IFOF) was performed using previously described ROIs[8]. A "two regions of interest" approach was used for each fasciculus tracking. The procedure[9] consisted in defining a second ROI, at a distance from the first ROI, such that it contained at least a section of the desired fasciculus but did not contain any fibres of the undesired fasciculus that passed through the first ROI. Fibre tracking was performed using a Diffusion Tensor model with a likelihood algorithm. A number of 5 points was put in each voxel of the ROIs used to track each fasciculus. At each tracking step, the algorithm moved the main tensor direction by 0.546875mm (default parameter in BrainVisa). Pathways were traced out until the fractional anisotropy of the tensor fell below an arbitrary threshold of 0.20.

For the SLF, a single ROI was used to visualise the entire arcuate fasciculus, then a two-ROIs approach was used to visualise subcomponents of the SLF[10]. For the two-ROI approach, the first ROI was placed in the white matter underlying Broca territory and the second ROI was drawn caudally including the white matter under the Geschwind and the Wernicke territory[10]. For the ILF, the first ROI was drawn in the occipital white matter and the second ROI was placed in the white matter underlying the rostral temporal regions[11]. For the IFOF, the first ROI was placed in the occipital white matter and the second ROI was drawn rostrally in the white matter of the anterior floor of the external capsule[8].

DTI and high-resolution 3-D anatomical images were registered using Brainvisa 3.0.2. The derived tracts were displayed using Anatomist 3.0.2 (http://brainvisa.info/) and indirect measurements of tract volumes were obtained by counting the number of streamlines for each tract in both hemispheres.

To explore more in detail in the present patients the possible involvement of the SLF[12-14], we also projected their lesions to the normalized white matter percentage maps of the SLF (ranging from 0 to 50%) based on DTI tractography of 16 normal subjects[15].

Case reports and supplementary results

Case 1 showed left motor deficit, left somatosensory extinction and dysarthria as a consequence of an ischemic stroke in the territory of the right middle cerebral artery, affecting both the inferior parietal and the superior temporal cortices (see Table 1 and Supplementary Figure 1). Despite the localization of the cortical lesion, nine days after clinical onset case 1 displayed no signs of extinction or neglect on neuropsychological testing.

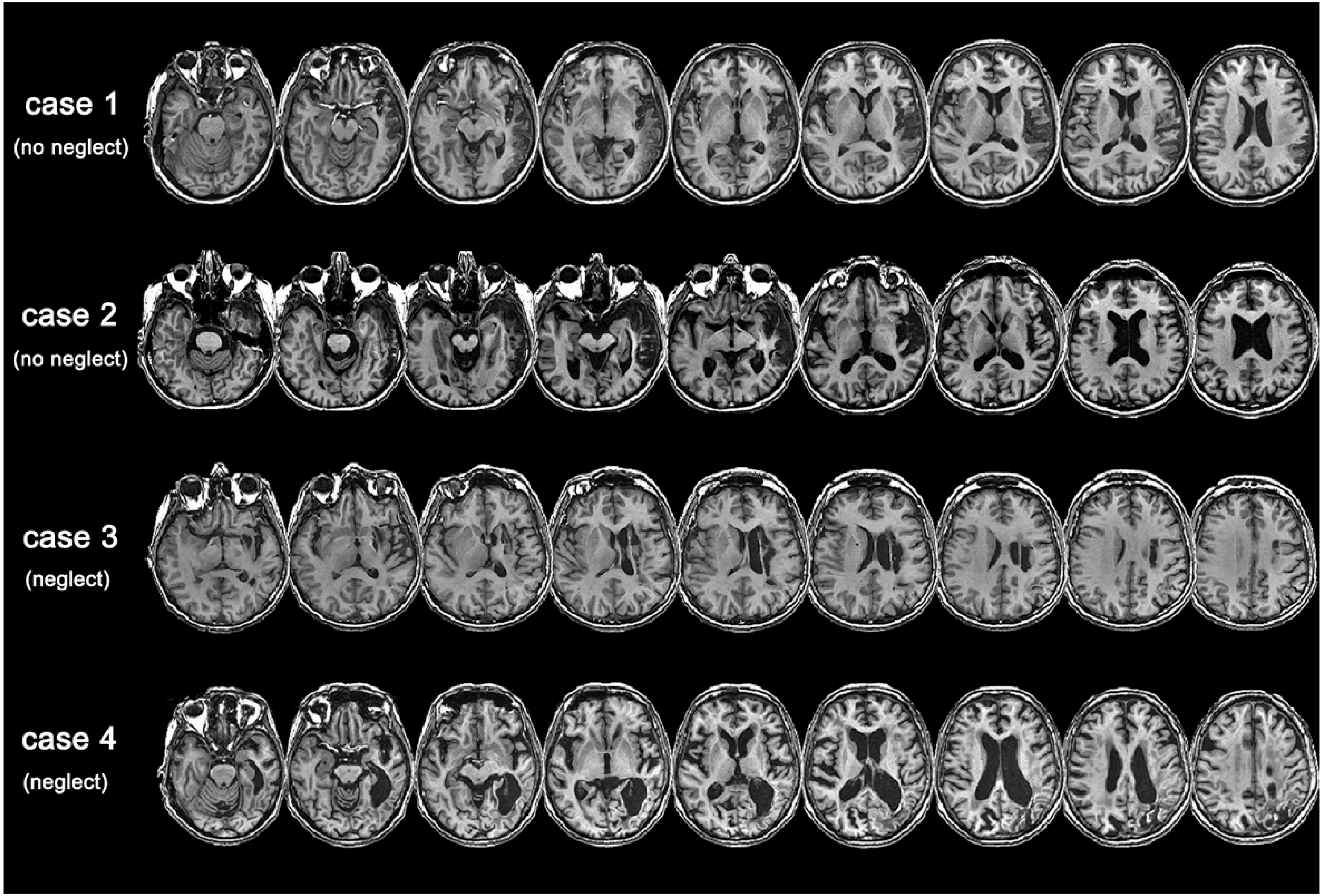

Supplementary Figure 1. MRI axial slices of the lesions in the right hemisphere for the four patients (neurological convention: left hemisphere is on the left side

Case 2 was admitted to hospital with dysarthria, left upper limb motor deficit, and extinction for left visual and tactile stimuli as a consequence of an ischemic stroke in the territory of the right middle cerebral artery affecting the temporal lobe (see Table 1 and Supplementary Figure 1). Five days later, a mild motor deficit persisted. Orientation in time and space was normal and there were no more signs of visual field deficit, sensory extinction or left neglect.

Case 3 was admitted to hospital with left hemiparesis predominant in the arm, left Babinski sign, rightward deviation of the head, signs of left neglect and anosognosia as a consequence of an ischemic stroke in the territory of the right middle cerebral artery (see Table 1 and Supplementary Figure 1). Nine days later, case 3 still had left visual and tactile extinction, signs of severe left neglect and anosognosia. When describing from memory of a map of France,[16] she produced 8 items on the left side and 7 items on the right side, thus showing no evidence of imaginal neglect[17]. At follow-up testing 34 days after clinical onset, case 3 still showed signs of left neglect. She found 2 targets on the left and 11 on the right on the bells cancellation test[5], 16 targets on the left and 29 on the right on the letter cancellation test[18], deviated rightward by 15% on line bisection[2], omitted the leftmost tree and the left extremity of the house on the landscape drawing copy[19], made no omission on the line cancellation[3] and on the overlapping figure tests[6], and showed left visual and tactile extinction. On further testing one week after, she performed in a similar manner. She found 2 targets on the left and 15 on the right on the bells cancellation test, 15 targets on the left and 25 on the right on the letter cancellation test, deviated rightward by 20% on line bisection, had identical performance on the landscape drawing, made no omission on the line cancellation and on the overlapping figure tests, and had left visual and tactile extinction.

Case 4 had a right hemorrhagic occipital-parietal stroke, which resulted in left homonymous hemianopia (see Table 1 and Supplementary Figure 1). A small medial occipito-parietal lesion was also present in the left hemisphere (Supplementary Figure 1). Two years after clinical onset, she had left hemiparesis and signs of left neglect. She was anosognosic and did not explore the left hemispace to compensate for her hemianopia. Neuropsychological examination revealed no deficit of memory or language.

The supplementary Table reports the number of streamlines for each fasciculus. The small number of streamlines in the left hemisphere of case 4 likely resulted from the concomitant left occipito-parietal lesion in this patient.

Supplementary Table. Number of streamlines for the three fascicles tracked in the left (L) and the right (R) hemisphere of each patient

	SLF		*IFOF*		*ILF*	
Case	*L*	*R*	*L*	*R*	*L*	*R*
1	796	575	286	165	2566	1041
2	25	693	47	248	1090	718
3	2051	1874	61	0	714	4684
4	365	991	4	0	608	3228

SLF, superior longitudinal fasciculus; IFOF, inferior fronto-occipital fasciculus; ILF, inferior longitudinal fasciculus

Supplementary Figure 2 illustrates how the lesions of cases 3 and 4, but not of cases 1 and 2, overlap with the likely normal localisation[20] of the SLF. This might suggest partial damage to the SLF in cases 3 and 4.

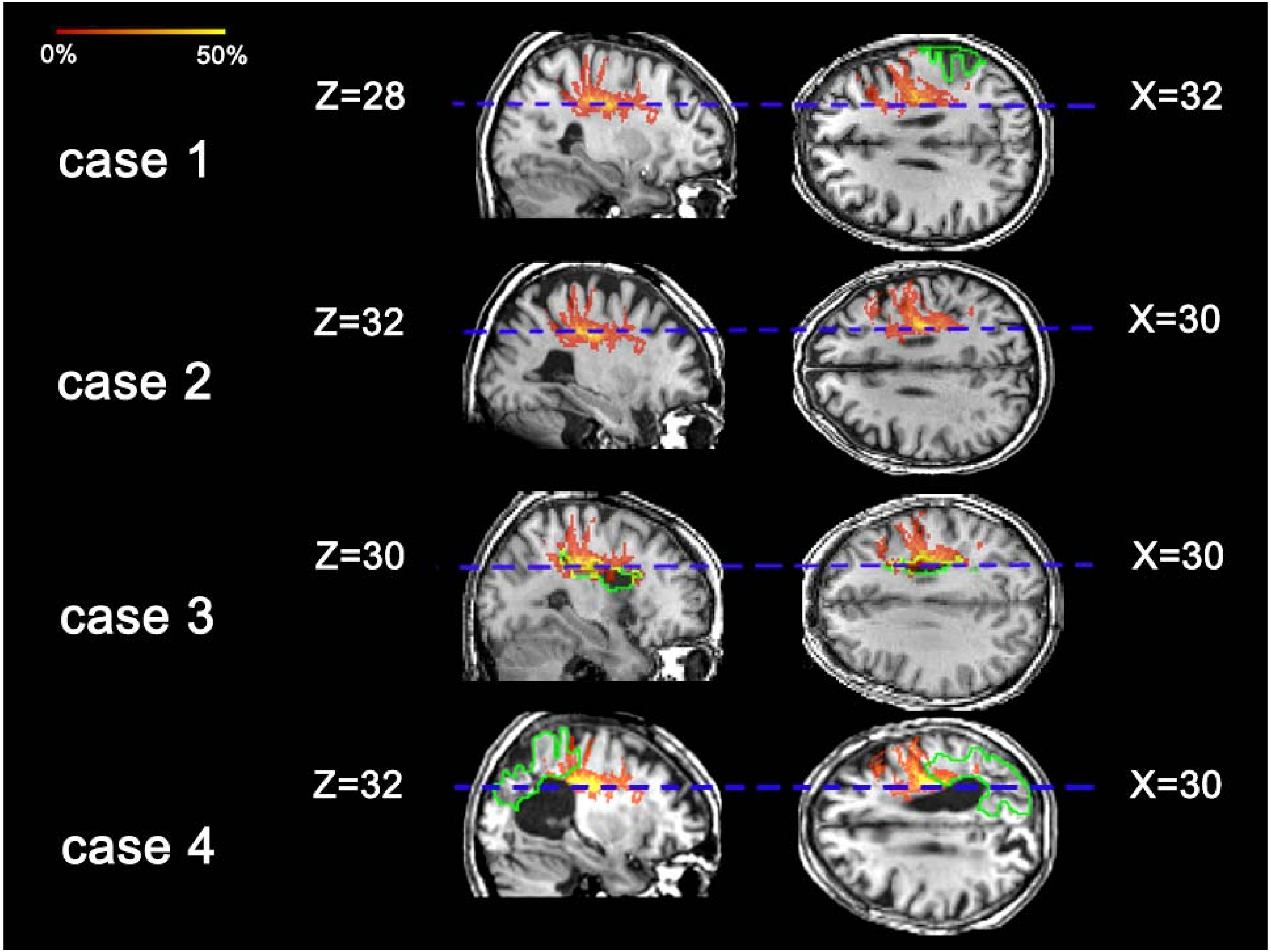
0%
50%
case 1
Z=28
X=32
case 2
Z=32
X=30
case 3
Z=30
X=30
case 4
Z=32
X=30

Supplementary Figure 2. Overlay of the patients' lesions (outlined in green) and of the normalized percentage maps of the SLF localisation (red-yellow colour scale) for 16 normal subjects[20] in the MNI referential space (http://www.mni.mcgill.ca). An axial and a sagittal MRI slices are shown for each patient. For case 2, there was no slice containing both the SLF and the lesion.

Supplementary references

1. Bartolomeo P, Chokron S. Egocentric frame of reference: Its role in spatial bias after right hemisphere lesions. Neuropsychologia 1999;37(8):881-894.
2. D'Erme P, De Bonis C, Gainotti G. Influenza dell'emi-inattenzione e dell'emianopsia sui compiti di bisezione di linee nei pazienti cerebrolesi [Influence of unilateral neglect and hemianopia on line bisection performance in brain-damaged patients]. Archivio di Psicologia, Neurologia e Psichiatria 1987;48:165-189.
3. Albert ML. A simple test of visual neglect. Neurology 1973;23:658-664.
4. Mesulam MM. Attention, confusional states and neglect. In: Mesulam MM, editor. Principles of Behavioral Neurology. Philadelphia (PA): F.A. Davis; 1985. p. 125-168.
5. Gauthier L, Dehaut F, Joanette Y. The bells test: A quantitative and qualitative test for visual neglect. International Journal of Clinical Neuropsychology 1989;11:49-53.
6. Gainotti G, D'Erme P, Bartolomeo P. Early orientation of attention toward the half space ipsilateral to the lesion in patients with unilateral brain damage. Journal of Neurology, Neurosurgery and Psychiatry 1991;54:1082-1089.
7. Mangin JF, Poupon C, Clark C, Le Bihan D, Bloch I. Distortion correction and robust tensor estimation for MR diffusion imaging. Medical Image Analysis 2002;6(3):191-198.
8. Catani M, Howard RJ, Pajevic S, Jones DK. Virtual in vivo interactive dissection of white matter fasciculi in the human brain. Neuroimage 2002;17(1):77-94.
9. Basser PJ, Pierpaoli C. A simplified method to measure the diffusion tensor from seven MR images. Magnetic Resonance in Medicine 1998;39(6):928-934.
10. Catani M, Jones DK, ffytche DH. Perisylvian language networks of the human brain. Annals of Neurology 2005;57(1):8-16.
11. Catani M, Jones DK, Donato R, Ffytche DH. Occipito-temporal connections in the human brain. Brain 2003;126(Pt 9):2093-107.
12. Bartolomeo P, Thiebaut de Schotten M, Doricchi F. Left unilateral neglect as a disconnection syndrome. Cerebral Cortex 2007:doi: 10.1093/cercor/bhl181.
13. Doricchi F, Tomaiuolo F. The anatomy of neglect without hemianopia: a key role for parietal-frontal disconnection? NeuroReport 2003;14(17):2239-2243.
14. Thiebaut de Schotten M, Urbanski M, Duffau H, Volle E, Lévy R, Dubois B, et al. Direct evidence for a parietal-frontal pathway subserving spatial awareness in humans. Science 2005;309(5744):2226-2228.
15. Thiebaut de Schotten M, Kinkingnéhun SR, Delmaire C, Thivard L, Lévy R, Volle E, et al. Visualization of disconnection syndromes in humans. submitted.
16. Rode G, Perenin MT. Temporary remission of representational hemineglect through vestibular stimulation. NeuroReport 1994;5:869-872.
17. Bartolomeo P, D'Erme P, Gainotti G. The relationship between visuospatial and representational neglect. Neurology 1994;44:1710-1714.
18. Mesulam MM. Principles of Behavioral Neurology. Philadelphia (PA): F.A. Davis; 1985.
19. Gainotti G, Messerli P, Tissot R. Qualitative analysis of unilateral spatial neglect in relation to the laterality of cerebral lesions. Journal of Neurology, Neurosurgery and Psychiatry 1972;35:545-550.
20. Thiebaut de Schotten M, Kinkingnéhun SR, Delmaire C, Lévy R, Volle E, Dubois B, et al. OVER-TRACK: A new tool to visualize the white matter organization in Talairach space. Neuroimage 2006;31(Supplement 1):S110.